Plasmonics (2015) 10:547–551
DOI 10.1007/s11468-014-9839-4

Extraordinary Optical Transmission of Broadband Through Tapered Multilayer Slits

Wan Zhang · Yongkai Wang · Lina Luo · Guian Li · Zhongyue Zhang

Received: 4 August 2014 / Accepted: 5 November 2014 / Published online: 19 November 2014

Abstract The nonresonant, enhanced optical transmission of subwavelength metallic slits on a thin film is significant in broadband light harvesting devices. To improve transmission efficiency, this paper established tapered multilayer slits in which thin dielectric layers are sandwiched between two metallic layers. The transmission properties of these slits are then investigated using the finite element method. Results show that transmission is improved in the tapered multilayer slits relative to that in the tapered monolayer slits. The effects of structural parameters on these transmission properties are also examined.

Keywords Extraordinary optical transmission · Surface plasmon polaritons · Tapered multilayer slits

Introduction

In 1998, Ebbesen et al. observed extraordinary optical transmission (EOT) in a metallic film perforated by a periodic array of subwavelength holes [1]. Hole arrays can achieve unexpectedly high transmission, although the diameter of a single isolated hole is much smaller than the wavelength of the incident light. Moreover, EOT is related to applications such as enhanced spectroscopy [2] and chemical or biological sensors [3, 4]. Thus, the study of the EOT of a metallic film with subwavelength holes has attracted much attention. Numerous researchers have designed various subwavelength nanoholes with different topologic shapes to enhance transmittance and to explore underlying physical mechanisms.

W. Zhang · Y. Wang · L. Luo · G. Li · Z. Zhang (✉)
School of Physics and Information Technology, Shaanxi Normal University, Xi'an 710062, China
e-mail: zyzhang@snnu.edu.cn

EOT phenomenon is mainly due to the match between the wavelength of surface plasmon polaritons (SPPs) and the period of the aperture array [5–12]. They are the surface electromagnetic waves of collective electron oscillations induced by the coupling of light with surface charges under the Bragg coupling condition [13],

$$\mathrm{Re}\left[\frac{\omega}{c}\sqrt{\frac{\varepsilon_m\varepsilon_d}{\varepsilon_m+\varepsilon_d}}\right] = \left|k_0\sin\alpha + iG_x + jG_y\right| \quad (1)$$

where ω, c, ε_d, ε_m, k_0, α, and (i, j) are the angular frequency, light speed, the relative permittivity of the dielectric material, the relative permittivity of the metal, the momentum of free-space light, the incident angle, and the order of specific SPP modes, respectively.

The localized surface plasmon (LSP) of the subwavelength hole also plays an important role in the EOT phenomenon [14–22]. It induces a strong EOT effect on metallic holes with highly acute angles [22]. Furthermore, the waveguided-mode resonance that is similar to Fabry–Pérot also enhances transmission in the slit because the slit can be considered as a metallic waveguide section. Both ends of this section are open to free space [23–25]. In sum, the resonant phenomena primarily caused by these EOT mechanisms with periodic slits or hole arrays display a narrow spectral bandwidth, which limits the range of application.

To overcome the limitations of this narrow bandwidth, many researchers have investigated the broadband transparency of nonresonant devices, such as rectangular apertures connected to narrower slits [26] and metallic grating devices with linearly tapered monolayer slits [27]. This study indicates that the tapered metal/dielectric/metal multilayer slits can enhance transmission more than the tapered monolayer slits in infrared when they operate under normal incidence. Transmission properties are strongly dependent on structural

parameters; therefore, these results can guide the design of near-field light harvesting devices with broadband and strong transmission capability. It can also improve understanding regarding the transmission properties of multilayer structures.

Structure and Computational Method

The tapered monolayer and multilayer slits are presented in Fig. 1a, b, respectively. The tapered monolayer and multilayer slits are 400 nm thick, have an entrance width (W_{in}) of 200 nm, and have an exit width (W_{out}) of 30 nm in all calculations. These slits also share period P. The SiO_2 layer (n=1.5) is sandwiched in between two Ag layers in tapered multilayer slits; the thickness of this layer is denoted by h and its height is represented by H.

The complex relative permittivity of Ag is obtained from [28]. The transmission properties are simulated using the three-dimensional, commercial finite element method (FEM) software COMSOL Multiphysics. Transmittance is defined as $T=P_{out}/P_{in}$, which is the ratio of output power to incident power.

Results and Discussion

Figure 2 shows the transmission spectra of the tapered monolayer and multilayer slits. P=400 nm, h=100 nm, and H=150 nm in the tapered multilayer slits. Transmittance spectrum of the tapered monolayer slits displays two peaks, namely, λ_{I0}=0.59 μm and λ_{II0}=1.13 μm. Moreover, broadband is transmitted in infrared. The transmittance spectrum of the tapered multilayer slits shows three peaks, that is, λ_I=

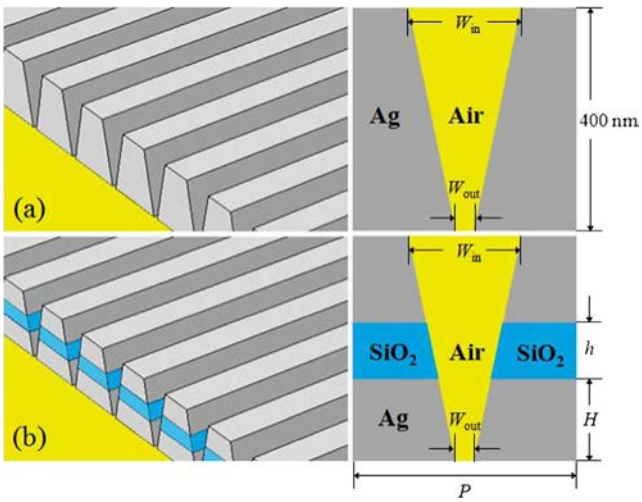

Fig. 1 Schematics of the tapered monolayer slits (**a**) and the tapered multilayer slits (**b**)

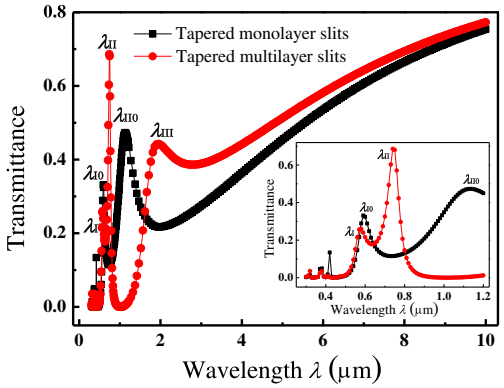

Fig. 2 Simulated transmission spectra of the tapered monolayer slits and the tapered multilayer slits

0.59 μm, λ_{II}=0.74 μm, and λ_{III}=1.96 μm, and its transmission in infrared is superior to that of the tapered monolayer slits.

To investigate the transmission mechanism, we examined the distributions (normalized by incident field amplitude E_0) of the electric field at the peaks and at the broadband of the transmission spectra of the tapered monolayer and multilayer slits, as depicted in Fig. 3a–g. The red arrows represent only the direction of the electric field. The "+" sign denotes positive charges, whereas the "–" sign corresponds to negative charges.

The electric fields of the tapered monolayer slits at λ_{I0}= 0.59 μm [Fig. 3a] are distributed into three parts: the slit entrance, the middle of the slit, and the slit exit. At λ_{II0}= 1.13 μm [Fig. 3b], the electric fields are distributed into two parts, namely, the entrance and the exit of the slit. At λ_{I0}= 0.59 μm and λ_{II0}=1.13 μm, the Fabry–Pérot-like resonance

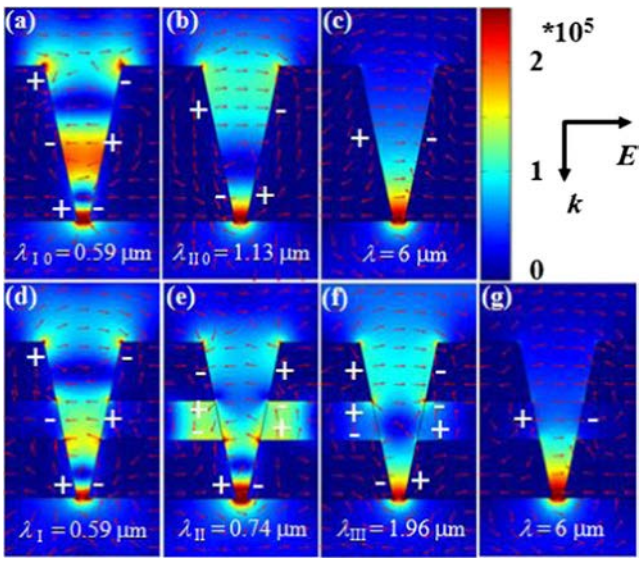

Fig. 3 Steady-state electric field distributions of the tapered monolayer slits [λ=0.59 μm (**a**), 1.13 μm (**b**), and 6 μm (**c**)] and the tapered multilayer slits [λ=0.59 μm (**d**), 0.74 μm (**e**), 1.96 μm (**f**), and 6 μm (**g**)]

occurs in the tapered monolayer slits. The current study sets the broadband transmission wavelength at λ=6 μm [Fig. 3c]. The positive charges gather on one side of the slit and the negative charges on the other. Furthermore, strong electric fields appear only at the exit of the slit. The tapered monolayer slits transmit nonresonantly in infrared.

At λ_I=0.59 μm [Fig. 3d], the electric field is distributed into three parts: the slit entrance, the middle of the slit, and the slit exit. This electric field distribution is similar to that of the tapered monolayer slits at λ_{I0} [Fig. 3a], which denotes the same resonant mode. At λ_{II}=0.74 μm [Fig. 3e], the electric fields in the vertical slit and in the dielectric layer are strong, and Fabry–Pérot-like resonances occur in these areas. These regions also constitute the resonant cavity. At λ_{III}=1.96 μm [Fig. 3f], the electric field is mainly distributed at the vertical slit. This distribution is similar to that of the tapered monolayer slits at λ_{II0}. When a layer dielectric spaces the tapered monolayer slits, additional charges gather at the entrance and the exit of the slit. The electron oscillation length of the resonant mode λ_{III} increases compared to the resonant mode λ_{II0}, so the position of the mode shows red shift. At λ=6 μm [Fig. 3g], the electric field distribution is similar to that of the tapered monolayer slits [Fig. 3c]. The tapered multilayer slits are modeled as a series of cascaded circuit. Given that the dielectric layer replaces some of the metal in the tapered monolayer slits, these slits are less impeded [27] than tapered monolayer slits are. Hence, the transmission of tapered multilayer slits is higher than that of the tapered monolayer slits.

Transmission properties may be affected by the thickness of the dielectric layer, the position of this layer, and the slits period given the paradigm structure of the tapered metal/dielectric/metal multilayer slits. The thickness h of the dielectric layer is enhanced from 50 to 250 nm with P=400 and H=150 nm to investigate the effect of h on the transmittance of tapered multilayer slits. The resonant transmission peak λ_I is insensitive to h as indicated in Fig. 4. The position of peak λ_{II} shows blueshift because the effective refractive index (n_{eff}) of the dielectric layer decreases as h increases, and n_{eff} is obtained using the model analysis solver of COMSOL Multiphysics. The position of peak λ_{III} shows red shift because electron oscillation length extends as h increases. The metal parts are reduced in the cascaded circuit as h increases. Hence, the impendence of the cascaded circuit decreases, and the transmittance at the nonresonant broadband increases. With the further increase of h, the transmission increases, and large electric fields gather at the exit of the slit. We calculated the difference between the tapered multilayer slits with h=350 nm and the tapered monolayer slits. The maximum transmission improvement is 26 % at λ=2.6 μm. With the further increases of λ, the improvement decreases monotonously, and the improvement is 8 % at λ=10 μm.

The dielectric layer is moved up by increasing H to investigate the effect of the location of the dielectric layer of the tapered multilayer slits on transmittance. Figure 5 shows the transmittance spectra of different H values with a fixed h=100 nm and P=400 nm. The transmission peak λ_{III} blueshifts slightly with the increase in H, and intensity decreases monotonously. Furthermore, the transmittance at the nonresonant broadband decreases.

We then investigate the effect of period P on the transmission of the tapered multilayer slits. Figure 6 presents the simulated transmission spectra of these slits with P=300, 400, and 500 nm at a fixed h=100 nm and H=150 nm. All of the resonant transmission peaks red shift with an increase in period as a result of the extension of the length of the dielectric layer cavity with P.

Previous studies on tapered multilayer slits consider only ideal and regular shapes. However, layers with ideal the multilayer slit locations are difficult to be fabricated experimentally. The two adjacent dielectric layers are initially restricted to equal variation; however, these layers can be varied independently during experiment. Thus, we determine the effect of asymmetric dielectric layers on the transmission properties of multilayer slits, and a potential scenario is depicted in Fig. 7a. For simplicity, the height of one dielectric layer is presumably fixed at H=150 nm, and the height H_V of

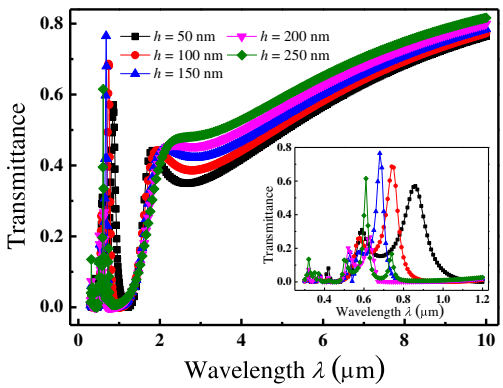

Fig. 4 Simulated transmission spectra of the tapered multilayer slits with different h values

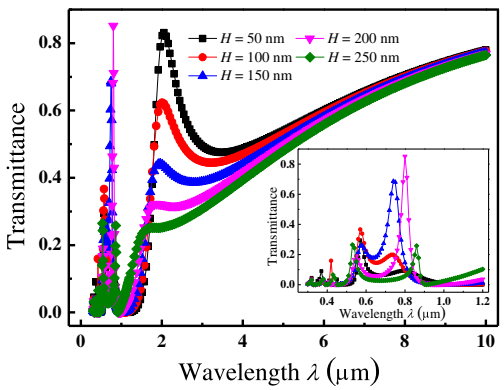

Fig. 5 Simulated transmission spectra of the tapered multilayer slits with different H values

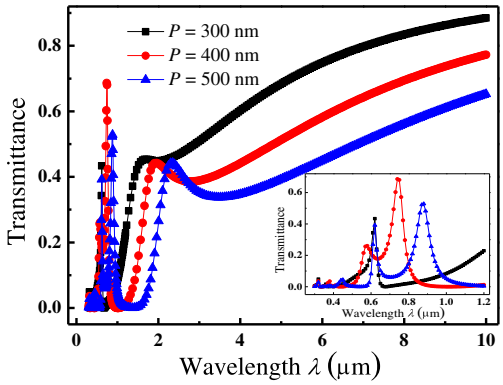

Fig. 6 Simulated transmission spectra of the tapered multilayer slits with different P values

the adjacent dielectric layer changes independently. The increase in H_V causes the transmission peaks λ_I, λ_{II}, and λ_{III} to shift slightly as in Fig. 7a and reduces the transmittance at λ_{III}. However, the transmittance does not vary significantly in the far infrared region with the different offset H_V.

The tapered multilayer slit is composed of upper and lower monolayer slits that are separated by a dielectric layer. Each monolayer slit can be fabricated independently during experimentation. Hence, the centers of these slits may not be aligned. This misalignment affects the transmission properties of the tapered multilayer slits as presented in Fig. 8a. The nonaligned structures are fixed at h=100 nm, H=150 nm, and P=400 nm. Furthermore, the two monolayers are separated by air with a refractive index of n=1. The deviation in the centers of

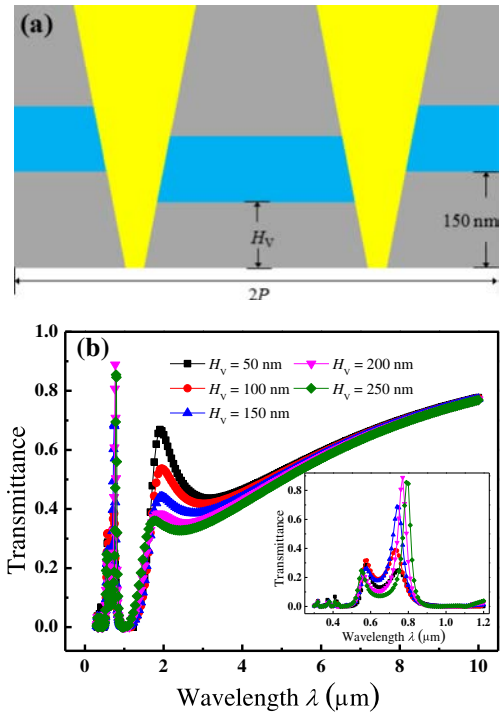

Fig. 7 (**a**) Schematic of the tapered multilayer slits with asymmetric layer heights; (**b**) Simulated transmission spectra of the tapered multilayer slits with different H_V values

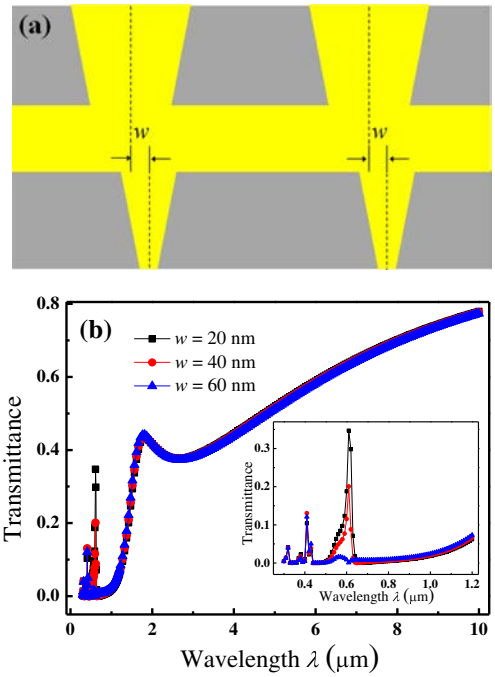

Fig. 8 (**a**) Schematic of the tapered multilayer slits in which the centers of two separated monolayer slits deviate; (**b**) Simulated transmission spectra of the tapered multilayer slits with different w values

the two monolayers is denoted by w. Although the transmittance of λ_I is decreased as suggested in Fig. 8b, the transmittance does not vary obviously with w. The transmittance at the nonresonant broadband decreases slightly with the increases in w.

The results exhibited in Figs. 7b and 8b imply that the asymmetry and the smaller deviation of the two separated monolayers do not alter the performance of broadband, and the enhanced transmission of the tapered multilayer slits obviously in the infrared region. This finding can thus guide the fabrication of such slits and their future applications in near-field optics.

Conclusions

This study proposes a paradigm structure of tapered multilayer slits to enhance transmittance relative to the tapered monolayer slits. In the tapered multilayer slits, the transmission spectra and the normalized electric field distribution are investigated using FEM. The results show that our structure generates a higher transmission in infrared than the tapered monolayer slits. The transmission properties are robust against the asymmetry, and deviation of the two separated monolayer slits although they are strongly dependent on the thickness and location of the dielectric layer. These results may be applied in near-field optics and may also enhance understanding regarding the transmission properties of multilayer structures.

Acknowledgments This work was supported by the National Natural Foundation of China (Grant no. 11004160) and the Fundamental Research Funds for the Central Universities (Grant no. GK201303007).

References

1. Ebbesen TW, Lezec HJ, Ghaemi HF, Thio T, Wolff PA (1998) Extraordinary optical transmission through sub-wavelength hole arrays. Nature 391:667–669
2. Gray SK (2007) Surface plasmon-enhanced spectroscopy and photochemistry. Plasmonics 2:143–146
3. Dahlin A, Zach M, Rindzevicius T, Kall M, Sutherland DS, Hook F (2005) Localized surface plasmon resonance sensing of lipid-membrane-mediated biorecognition events. J Am Chem Soc 127: 5043
4. Karabchevsky A, Krasnykov O, Auslender M, Hadad B, Goldner A, Abdulhalim I (2009) Theoretical and experimental investigation of enhanced transmission through periodic metal nanoslits for sensing in water environment. Plasmonics 4:281–292
5. Shahmansouri A, Rashidian B (2013) Enhanced optical transmission through metallic holes array: role of TE polarization in SPP excitation. Plasmonics 8:403–409
6. Wang YK, Qin Y, Zhang ZY (2014) Extraordinary optical transmission property of X-shaped plasmonic nanohole arrays. Plasmonics 9: 203–207
7. Huang LL, Chen XZ, Bai BF, Tan QF, Jin GF, Zentgraf T, Zhang S (2013) Helicity dependent directional surface plasmon polariton excitation using a metasurface with interfacial phase discontinuity. Light: Sci Appl 2:e70
8. Ghaemi HF, Thio T, Grupp DE, Ebbesen TW, Lezec HJ (1998) Surface plasmons enhance optical transmission through subwavelength holes. Phys Rev B 58:6779–6782
9. Holman ZC, Wolf SD, Ballif C (2013) Improving metal reflectors by suppressing surface plasmon polaritons: a priori calculation of the internal reflectance of a solar cell. Light: Sci Appl 2:e106
10. Genet C, Ebbesen TW (2007) Light in tiny holes. Nature 445:39
11. Barnes WL, Murray WA, Dintinger J, Devaux E, Ebbesen TW (2004) Surface plasmon polaritons and their role in the enhanced transmission of light through periodic arrays of subwavelength holes in a metal film. Phys Rev Lett 92:107401
12. Sun Q, Ueno K, Yu K, Kubo A, Matsuo Y, Misawa H (2013) Direct imaging of the near field and dynamics of surface plasmon resonance on gold nanostructures using photoemission electron microscopy. Light: Sci Appl 2:e118
13. Ortuño R, García-Meca C, Rodríguez Fortuño FJ, Martí J, Martínez A (2009) Role of surface plasmon polaritons on optical transmission through double layer metallic hole arrays. Phys Rev B 79:075425
14. Najiminaini M, Vasefi F, Kaminska B, Carson JJL (2013) A three-dimensional plasmonic nanostructure with extraordinary optical transmission. Plasmonics 8:217–224
15. Klein Koerkamp KJ, Enoch S, Segerink FB, van Hulst NF, Kuipers L (2004) Strong influence of hole shape on extraordinary transmission through periodic arrays of subwavelength holes. Phys Rev Lett 92: 183901
16. Gordon R, Brolo AG, McKinnon A, Rajora A, Leathem B, Kavanagh KL (2004) Strong polarization in the optical transmission through elliptical nanohole arrays. Phys Rev Lett 92:037401
17. Degiron A, Ebbesen TW (2005) The role of localized surface plasmon modes in the enhanced transmission of periodic subwavelength apertures. J Opt A Pure Appl Opt 7:S90–S96
18. Parsons J, Hendry E, Burrows CP, Auguié B, Sambles JR, Barnes WL (2009) Localized surface-plasmon resonance in periodic nondiffracting metallic nanoparticle and nanohole arrays. Phys Rev B 79:073412
19. Lovera P, Jones D, Corbett B, O'Riordan A (2012) Polarization tunable transmission through plasmonic arrays of elliptical nanopores. Opt Express 20:25325
20. Bao YJ, Peng RW, Shu DJ, Wang M, Lu X, Shao J, Lu W, Ming NB (2008) Role of interference between localized and propagating surface waves on the extraordinary optical transmission through a subwavelength-aperture array. Phys Rev Lett 101:087401
21. Lin L, Roberts A (2011) Light transmission through nanostructured metallic films: coupling between surface waves and localized resonances. Opt Express 19:2626–2633
22. Rodrigo SG, Mahboub O, Degiron A, Genet C, Garcia-Vidal FJ, Martin-Moreno L, Ebbesen TW (2010) Holes with very acute angles: a new paradigm of extraordinary optical transmission through strongly localized modes. Opt Express 18:23691–23697
23. Xu JJ, Guan P, Kvasnicka P, Gong H, Homola J, Yu QM (2011) Light transmission and surface-enhanced Raman scattering of quasi-3D plasmonic nanostructure arrays with deep and shallow Fabry-Perot nanocavities. J Phys Chem C 115:10996–11002
24. Ruan Z, Qiu M (2006) Enhanced transmission through periodic arrays of subwavelength holes: the role of localized waveguide resonances. Phys Rev Lett 96:233901
25. Marani R, Marrocco V, Grande M, Morea G, D'Orazio A, Petruzzelli V (2011) Enhancement of extraordinary optical transmission in a double heterostructure plasmonic bandgap cavity. Plasmonics 6: 469–476
26. Subramania G, Foteinopoulou S, Brener I (2011) Nonresonant broadband funneling of light via ultrasubwavelength channels. Phys Rev Lett 107:163902
27. Shen HH, Maes B (2012) Enhanced optical transmission through tapered metallic gratings. Appl Phys Lett 100:241104
28. Johnson PB, Christy RW (1972) Optical constants of the noble metals. Phys Rev B 6:4370–4379